# Time-Resolved Continuum-Edge-Shift Measurements in Laser-Shocked Solids

D. K. Bradley,[1] J. Kilkenny,[3] S. J. Rose,[2] and J. D. Hares[1]
[1]*Imperial College, London, England*
[2]*Rutherford Appleton Laboratory, Didcot, England*
[3]*Lawrence Livermore National Laboratory, University of California, Livermore, California 94550*
(Received 24 July 1987)

The first measurements of the shift in position of the photoabsorption edge in a laser-heated and shocked solid material are reported. A buried tracer layer is first radiatively heated to a few electronvolts leading to the appearance of bound-bound transitions near to the $K$ photoabsorption edge. Then as the shock runs through, the $K$ edge shifts to lower energy ionizing the bound-bound transitions, in agreement with theory.

PACS numbers: 78.70.Dm, 79.20.DS

High-power lasers can be used to produce high material densities and pressures, such as occur in the center of stars[1] and in proposed inertial-containment fusion compressions. Although measurements of the velocity of shocks driven by high-power lasers have been made,[2] detailed measurements of the electronic structure of the dense shocked plasmas have not to our knowledge been attempted. This is because the dense plasma is generally not hot enough for self-emission to be a viable technique. Under such conditions, absorption spectroscopy is a promising alternative. Previous work[3] has used an implosion to provide flash x-ray backlighting of its own hot imploding shell. Here we use a 0.9-nsec laser-produced x-ray backlighter and an x-ray streak spectrometer to yield true time resolution of the evolution of structure at the photoabsorption edge of a relatively homogeneous tracer layer.

The structure and position of the photoabsorption edges in a plasma depends on several effects, namely a change in the electronic shielding of inner shells[4] due to ionization, continuum-lowering[5] depression, and electron degeneracy. Measurements of the edge shift have, in general, been limited to emission from high-temperature plasmas at densities low compared to solid densities.[6] In this paper we observe the properties of the $K$ photoabsorption edge of chlorine as it is radiatively preheated to a temperature of several electronvolts and is then compressed by a strong shock to several times solid density.

Novel features are observed. First, structure appears at the edge as the chlorine is heated. This is attributed to $1s$-$3p$ absorption made possible by vacancies in the $3p$ level of the heated KCl. We suggest that this feature could be used to diagnose the temperature of a plasma. Then at the time that the shock passes through the tracer layer, there is a red shift of the $K$ photoabsorption edge of $8 \pm 4$ eV which results in the $3p$ level no longer being bound; that is to say it has been pressure ionized. These are the first measurements known to us where depression of the ionization potential is demonstrated as the density of a plasma is increased above solid densities. We present results of a novel model that predicts the shift of the edge, in agreement with experiment.

These experiments were conducted at the United Kingdom Science and Engineering Research Council's Central Laser Facility. A laser beam of pulse duration 0.9 nsec, 0.53-$\mu$m wavelength, was focused to 60–100-$\mu$m-diam spots, giving irradiances of $5\times10^{14}$–$2\times10^{15}$ W/cm$^2$. The targets were layered consisting of 1-$\mu$m Bi, a variable thickness of polyester, 5-$\mu$m KCl, and 10-$\mu$m parylene-N. The laser was incident on the Bi-coated side producing a bright quasicontinuum of x-rays that had a time history that approximately followed the 0.9-nsec laser pulse. This emission was used to backlight the $K$ edge of the Cl in the KCl layer during its heating and compression.

The absorption spectrum of the Cl was measured by a focusing x-ray time-resolving crystal spectrometer that viewed the Bi emission through the layered target. The flux-gathering properties of this crystal allowed a high dispersion to be used (7 eV/mm), with a measured spectral resolution of 3 eV. The time resolution was limited to 30 psec by the time-resolving slit of the x-ray streak camera. Time-integrating crystal spectrometers at 45° and 135° to the target normal also recorded the x-ray emission. An optical streak camera focused onto the rear of the target simultaneously observed the time of the shock breakout from the rear of the target on some shots.

By our varying the thickness of the polyester in the target, both the heating of the KCl tracer layer and the time of arrival of the laser-driven strong shock (that has a rise time[2] of less than 0.1 nsec) at the tracer layer could be varied. We can categorize our data by three types of shot (a, b, and c) in increasing order of the heating of the KCl tracer layer as shown in Table I. Case a represents the smallest amount of heating where there was 25 $\mu$m of polyester to screen the tracer layer from the x-ray and shock heating. This results in an x-ray absorption profile of the Cl $K$ edge that does not change during the 0.9-nsec observation time. Case b has a

 

TABLE I. Categories of experiment in increasing order of heating of the KCl. The temperatures and change in the degree of ionization $\Delta Z$ are given at the end of the 0.9-nsec pulse for cases a and b, but in the middle of the pulse for case c just before the shock breaks through.

| Type | Laser energy (J) | Focal spot ($\mu$m) | Thickness of polyester shielding-layer ($\mu$m) | Calculated KCl heating ($10^5$ J/g) | Calculated $T$ (eV) | Calculated $\Delta Z$ | Observed $K$-edge energy (eV) |
|---|---|---|---|---|---|---|---|
| a | 15 | 120 | 25 | 0.6–1.6 | 4.5–8.0 | 0.3–0.7 | 2820–2824 |
| b | 19 | 125 | 10 | 0.9–3.0 | 6–13 | 0.4–1.2 | 2616–2824 |
| c | 15 | 85 | 10 | 0.9–3.0 | 6–13 | 0.4–1.2 | 2813–2822 |

slightly defocused laser spot, but only 10 $\mu$m of polyester to screen the tracer layer. The effect of x-ray heating is seen in this case, but the laser-driven shock does not reach the tracer layer within 0.9 nsec. Case c represents the smallest focus of the laser spot, where not only is the tracer layer heated by x rays, but the laser-driven shock also passes through the layer while the x rays are still being emitted from the Bi plasma. Simultaneous observation of the rear of the target showed that the shock breaks out at 1.1 nsec with a measured rise time of 0.07 nsec, in case c implying transit through the KCl tracer layer at 0.7 nsec. In cases a and b the shock breakout time implies transit throught the KCl at a time later than 1 nsec.

The time-integrated data from shots in categories a, b, and c are shown in Fig. 1. The absolute wavelength scale of the spectra was established by our measuring the wavelengths of some of the Bi lines[7] on separate shots. This allowed us to identify and fix the Ni-like (core)$3d_{3/2}^3 3d_{5/2}^6 4f_{5/2}$-(core) $3d_{3/2}^4 3d_{5/2}^6$ (herein abbreviated to $3\bar{d}_{3/2}4f_{5/2}$) and (core) $3d_{3/2}^4 3d_{5/2}^5 4f_{7/2}$-(core) $3d_{3/2}^4 3d_{7/2}^6 (3\bar{d}_{5/2}4f_{7/2})$ transitions of Bi at $2961 \pm 2$ eV and $2853 \pm 2$ eV, respectively. The Ni-like Bi $3\bar{d}_{5/2}4f_{7/2}$ transition is close to the Cl $K$ photoabsorption edge and acts as a convenient secondary wavelength in both the time-integrated and time-resolved data. Both lines are evident in Fig. 1.

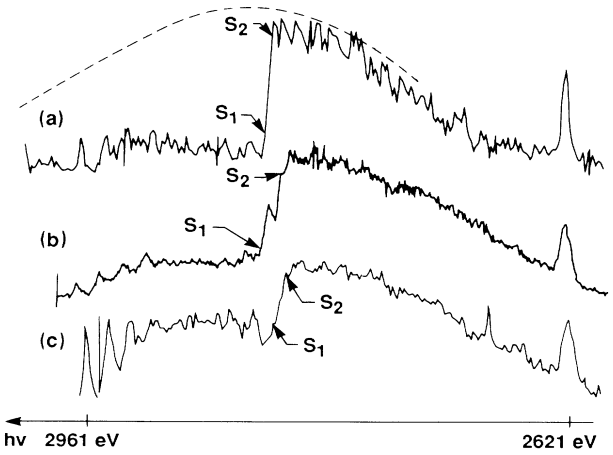


FIG. 1. Time-integrated spectra from the rear of the target showing the Cl $K$ photoabsorption edge for categories of increasing heating of KCl, a, b, and c (see text). The ordinate is x-ray transmission. The Bi fiducial lines $3d_{3/2}4f_{5/2}$ (2961 eV) and the Cl $K\alpha$ line (2621 eV) are marked. The shoulders of the edge are marked $S_1$ and $S_2$ and are at 2824, 2820 eV; 2824, 2816 eV; 2822, 2813 eV for cases a, b, and c, respectively. The spectrum recorded by the front spectrometer is sketched (broken line) on a only.

Figure 1(a) shows time-integrated data from the lowest-temperature case (category a) with a 25-$\mu$m layer of polyester. The $K$ edge lies between 2820 and 2824 eV (10% and 90% points), its width being due to spatial broadening by the 80-$\mu$m focal spot. Previous high-resolution measurements[8] of the edge in KCl have shown a fine structure associated with the bound levels and an edge at $2826 \pm 3$ eV.

In Fig. 1(b), a time-integrated spectrum from an experiment in category b is shown. A broadened and red-shifted edge between 2816 and 2824 eV is seen (marked $S_2$ and $S_1$), with a superimposed absorption line at 2819 eV. A spectrum from case c with the highest-temperature KCl absorber is shown in Fig. 1(c). The absorption line appears smeared out in these time-integrated data, and the edge is red shifted and broadened lying between 2815 and 2823 eV, an average shift of $-3$ eV.

The time-integrated spectra allow us to estimate the radiative heating of the KCl. X-ray spectra were recorded from the Bi between 1.9 and 3.5 keV. This is the region most effective in heating the buried KCl as softer parts of the spectrum are absorbed in the polyester. The film calibration[9] and the Bragg reflection integral[10] give the absolute x-ray spectrum. Using the cold mass absorption coefficients we calculate the temperature rise in different parts of the layered target due to radiative heating. For the cases a, b, and c, we calculate from the measured spectrum the spatially averaged and time-integrated x-ray heating in the KCl of approximately $1.1 \times 10^5$, $1.8 \times 10^5$, and $3.6 \times 10^5$ J/g, respectively.

The streaked data show the evolution of the $K$ edge more clearly because of the higher spectral resolution and the time resolution. A single lineout from the "cold" case a is shown in Fig. 2(a). The edge between 2822 and 2825 eV shows no shift during the 1 nsec of the streak. The jump ratio calculated from the film calibration and the initial areal density of the layer, is consistent with the cold opacity values.

For the higher-temperature cases, cases b and c, the edge position does change with time. Streaked spectra for case b are shown in Fig. 2(b). An absorption line, arguably a doublet, appears below the edge at 2819 eV and grows during the laser pulse. The case with the highest-temperature KCl absorber, case c, is illustrated in the sequence of Fig. 2(c). At early times a sharp edge is seen at the cold position. Up to 500 psec an absorption line grows below the edge as seen in the second lineout, and then at 700 psec the absorption line disappears and the edge shifts to between 2811 and 2821 eV, an average red shift of $-7$ eV. This time coincides with the inferred arrival of the laser-driven shock.

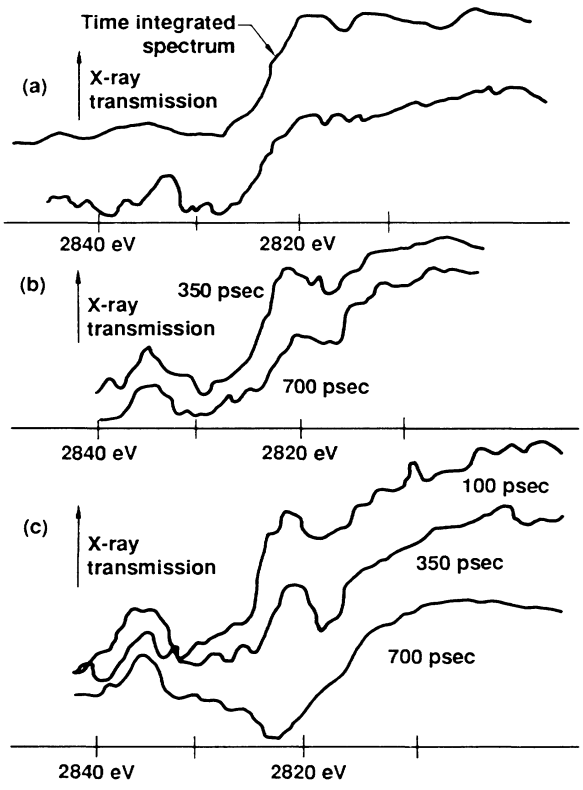


FIG. 2. Time-resolved spectra for categories of increasing heating a, b, and c (see text). (a) The "cold" case, with no temporal variation with the time-integrated spectrum of Fig. 1, case a, superimposed. (b) The medium heating case with the $1s-3p$ absorption feature ($Cl^+$ is calculated to be at 2819 eV) evolving. (c) The $1s$-$3p$ feature evolving (350 psec) and then ionized at 700 psec with a red shift of the edge. The wavelength scale is established by the Bi $3d_{5/2}4f_{7/2}$ line, not shown. In (b) and (c) there is a vertical displacement of the traces at different times for ease of display.

Thomas-Fermi[11] calculations for KCl have been performed in which the ion sphere radii for K and Cl Thomas-Fermi calculations are adjusted until the electronic pressures at the boundaries of the K and Cl spheres are equal. From these calculations the change in the average ionization of the chlorine and the temperature of KCl as a function of the energy deposition have been calculated and are shown in Fig. 3. At the end of the pulse in case b and in the middle of the pulse in case c, the above estimates of the radiative energy deposition give a KCl temperature ranging from 13 eV in the front to 6 eV at the back of the KCl, and a change in the average chlorine ionization of between 0.4 and 1.2. At the end of the pulse in case a, the temperature and the change in the chlorine ionization range between 4.5 and 8 eV and between 0.3 and 0.7, respectively.

Dirac-Fock calculations[12] of the average-of-configuration $1s$-$3p$ transition energies for Cl, $Cl^+$, and $Cl^{++}$ give 2816, 2819, and 2822 eV, respectively, to an accuracy of a few electronvolts. The observation of an absorption line appearing at 2819 eV (Figs. 1 and 2) suggests that $Cl^+$ is the dominant state of ionization at the end of the laser pulse in case b and at the middle of the laser pulse in case c, consistent with the Thomas-Fermi estimate of the change in the degree of ionization. In case a, the $1s$-$3p$ line is not seen consistent with the low degree of chlorine ionization predicted (a $1s$-$3p$ transition cannot occur in the $Cl^-$ ion).

We have also calculated the position of the $K$ edge in the Cl. We calculate the shift of the $K$ edge as the sum of three terms. The first term, $I_k$, is the average Cl $K$-shell ionization energy of an isolated atom (calculated with Dirac-Fock theory[12]) at the state of ionization appropriate to the plasma density and temperature taken from Thomas-Fermi theory. The second term, $E_{cl}$, represents the continuum lowering from the effect of plasma neighbors on the $K$-edge position and is approximated by

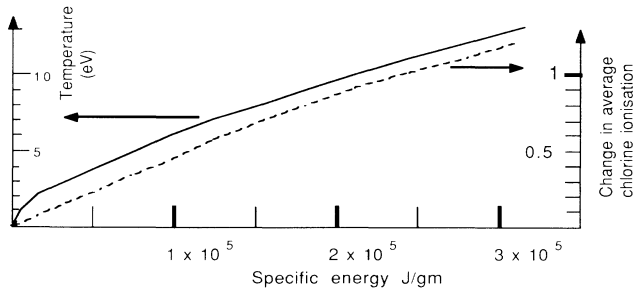


FIG. 3. Calculated change in degree of ionization of Cl in KCl and temperature of KCl as a function of energy deposition at solid density.

an ion sphere model.[5] The third term, $E_{deg}$, represents the partial degeneracy of the free-electron states close to the ionization energy.[1]

The method gives a shift of the $K$-edge position prior to the shock running into the KCl in case c (1.98 g/cm$^3$, 9 eV) of only 0.5 eV, comprising $\Delta I_K = +15.6$ eV, $\Delta E_{cl} = -9.0$ eV, $\Delta E_{deg} = -6.1$ eV. To find values for density and temperature after the shock, we have used a one-dimensional code,[13] and varied the ablation pressure to fit the observed shock breakout time. This code verifies that electron conduction is negligible as a heating mechanism for our tracer layers. With these values of density and temperature (6.2 g/cm$^3$, 19 eV) the shift is $-3.7$ eV comprising $\Delta I_K = 47.6$ eV, $\Delta E_{cl} = -45.2$ eV, $\Delta E_{deg} = -6.1$ eV. This is in fairly good agreement with the experimental observation and would imply that in cases b and c, the $3p$ level will exist before the shock but is pressure ionized after the shock passes through.

Lacking any appropriate theory for broadening of photoabsorption edges in such a dense plasma, we presume that our edge width is due to Stark broadening as well as gradients in the temperature and density through the layer. A nearest-neighbor approximation to the distribution gives an edge width of $0.76E_{cl}$.[14] As the continuum lowering is 45 eV, this simple treatment gives too large a value for the width of the edge. We suggest that this is because of the assumption of an uncorrelated distribution. Correlation would presumably narrow the width of the distribution of nearest neighbors to more closely approximate the experimental data.

In conclusion, we have measured the chlorine $K$-shell absorption spectrum in a laser-shocked KCl tracer layer. The appearance of a $1s$-$3p$ absorption line suggests that it may be used as a diagnostic of the state of ionization and hence temperature of a warm plasma. When the plasma is shocked to a density above that of the solid we observe the pressure ionization of the $3p$ level as the $K$ edge shifts to a lower energy. This edge shift is explained by a simple model as the difference between two larger effects, the energy increase from ionization and the decrease from continuum depression.

The assistance of A. J. Rankin with the optical streak camera measurements and the staff of the Vulcan laser is gratefully acknowledged. The work was performed under the auspices of the U.S. Department of Energy by the Lawrence Livermore National Laboratory under Contract No. W-7405-ENG-48.

[1]J. P. Cox, *Principles of Stellar Structure* (Gordon and Breach, New York, 1968), Vol. 1.

[2]R. J. Trainor, J. W. Shaner, J. M. Auerbach, and N. C. Holmes, Phys. Rev. Lett. **42**, 1154 (1979).

[3]A. Hauer, R. D. Cowan, B. Yaakobi, O. Barnouin, and R. Epstein, Phys. Rev. A **34**, 411 (1986).

[4]J. C. Slater, *Quantum Theory of Atomic Structure* (McGraw-Hill, New York, 1960), Vol. 1.

[5]J. Stewart and K. Pyatt, Astrophys. J. **144**, 1203 (1966).

[6]J. D. Kilkenny, R. W. Lee, M. H. Key, and J. G. Lunney, Phys. Rev. A **22**, 2746 (1980), and references therein.

[7]J. D. Kilkenny, "A Semi-Empirical Scaling of the Bright 3-4 Transitions of Laser-Produced High-Z Element" (to be published).

[8]L. G. Paratt and E. L. Jossem, Phys. Rev. **97**, 916 (1955); S. T. Stephenson, R. Krogstad, and W. Nelson, Phys, Rev. **84**, 806 (1951).

[9]B. L. Henke, F. G. Fujiwara, M. A. Tester, C. H. Dittmore, and M. A. Palmer, Opt. Soc. Am. B **1**, 828 (1984).

[10]B. L. Henke and P. A. Jaanimagi, Rev. Sci. Instrum. **56**, 1538 (1985).

[11]R. P. Simon, N. Metropolis, and E. Teller, Phys. Rev. **75**, 1561 (1949).

[12]I. P. Grant, B. J. McKenzie, P. H. Norrington, D. F. Mayers, and N. C. Pyper, Comput. Phys. Commun. **21**, 207 (1980); B. J. McKenzie, I. P. Grant, and P. H. Norrington, Comput. Phys. Commun. **21**, 233 (1980).

[13]J. P. Christiansen, D. E. T. F. Ashby, and K. V. Roberts, Comput. Phys. Commun. **7**, 271 (1974).

[14]S. Davidson, J. Foster, S. Rose, C. L. Smith, and K. Wharbutton, Appl. Phys. Lett. (to be published), and Rutherford Laboratory Annual Report No. RAL 83-043, 1983 (unpublished), p. 54.